A single centre water splitting dye complex adsorbed on rutile TiO2(110): Photoemission, x-ray absorption, and optical spectroscopy

Matthew Weston, Thomas J. Reade, Andrew J. Britton, Karsten Handrup, Neil R. Champness, and James N. O'Shea

Citation: The Journal of Chemical Physics **135**, 114703 (2011); doi: 10.1063/1.3637497
View online: http://dx.doi.org/10.1063/1.3637497
View Table of Contents: http://scitation.aip.org/content/aip/journal/jcp/135/11?ver=pdfcov
Published by the AIP Publishing

A single centre water splitting dye complex adsorbed on rutile TiO_2(110): Photoemission, x-ray absorption, and optical spectroscopy

Matthew Weston,[1,2] Thomas J. Reade,[3] Andrew J. Britton,[1,2] Karsten Handrup,[1,2] Neil R. Champness,[3] and James N. O'Shea[1,2,a)]
[1]*School of Physics and Astronomy, University of Nottingham, NG7 2RD Nottingham, United Kingdom*
[2]*Nottingham Nanotechnology and Nanoscience Centre (NNNC), University of Nottingham, NG7 2RD Nottingham, United Kingdom*
[3]*School of Chemistry, University of Nottingham, NG7 2RD Nottingham, United Kingdom*

(Received 15 July 2011; accepted 22 August 2011; published online 19 September 2011)

A single centre water splitting dye complex (aqua(2,2′-bipyridyl-4,4′-dicarboxylic acid)-(2,2′:6′,6″-terpyridine)Ruthenium(II)), along with a related complex ((2,2′-bipyridyl-4,4′-dicarboxylic acid)-(2,2′:6',6″-terpyridine)chloride Ruthenium(II)), has been investigated using photoemission and compared to molecules with similar structures. Dye molecules were deposited *in situ* using ultra-high vacuum electrospray deposition, which allows for the deposition of thermally labile molecules, such as these dye molecules. Adsorption of the dye molecules on the rutile TiO_2(110) surface has been studied using core-level and valence photoemission. Core-level photoemission spectra reveal that each complex bonds to the surface via deprotonation of its carboxylic acid groups. A consideration of the energy level alignments reveals that both complexes are capable of charge transfer from the adsorbed molecules to the conduction band of the rutile TiO_2 substrate. © *2011 American Institute of Physics*. [doi:10.1063/1.3637497]

I. INTRODUCTION

Hydrogen gas has the potential to be used as a carbon neutral fuel with a high enough energy density to be used as a transportation fuel,[1] once a suitable storage medium has been found.[2–6] Hydrogen gas can be produced from several different processes;[7–9] however, they usually require some form of external power source to provide enough energy for the reaction. The most sustainable way of generating the energy would be from renewable energy sources, such as solar or wind power. The hydrogen production process could be made more efficient by merging the energy harvesting and water splitting processes into a combined system, potentially reducing energy losses from power transmission between the systems and simplifying manufacture.

Dye sensitised solar cells (DSCs) consist of efficient light harvesting molecules adsorbed onto the surface of a substrate with a wide bandgap, such as TiO_2.[10–12] After the molecule absorbs a photon of visible light, an electron is promoted from the highest occupied molecular orbital (HOMO) to the lowest unoccupied molecular orbital (LUMO), if this orbital overlaps energetically with the conduction band of the substrate then charge transfer from the molecule to the substrate can occur. After charge transfer has occurred the adsorbed molecule is left in a state which can accept electrons from another source. In a photovoltaic DSC, the lost electron is replaced either from a liquid electrolyte or from an adsorbed layer of gold on the substrate.[13,14] In a water splitting DSC, the loss of electrons creates a potential that causes the oxidation of a water molecule attached to the metal centre of the adsorbed dye molecule, leading to the production of H^+ ions. The process takes several steps and produces H^+ ions which travel to the cathode where they recombine with the electrons initially transferred to the substrate producing hydrogen molecules. Gold is probably not a suitable substrate for the reaction due to its ability to transfer electrons *to* adsorbed molecules,[14–16] this process would compete with the removal of electrons from the water molecules and reduce the efficiency of the water splitting reaction. Titanium dioxide, on the other hand, shows only efficient charge transfer *from* the adsorbed molecules to the substrate making it an ideal substrate for a water splitting DSC.[17–19]

The molecules studied in this work each contain a single bi-isonicotinic acid ligand (2,2′-bipyridyl-4,4′-dicarboxylic acid), these ligands have carboxylic acid groups which are capable of bonding to the TiO_2 surface. Bi-isonicotinic acid has previously been shown to adopt a 2M-bidentate structure when adsorbed to the rutile TiO_2(110) surface,[20] on adsorption the carboxylic acid groups deprotonate to allow the molecule to bond covalently to the surface. N3, the full name of which is cis-bis(isothiocyanato)bis(2,2′-bipyridyl-4,4′-dicarboxylato)-ruthenium(II), is currently one of the most efficient dye complexes used in photovoltaic DSCs and contains two bi-isonicotinic acid ligands which allow it to bond to the TiO_2 surface.[21] Previous studies of N3 and related molecules on rutile TiO_2(110) using photoemission spectroscopy have shown evidence of deprotonation of two carboxylic acid groups on adsorption to the TiO_2 surface for each of the molecules studied.[18,19,22] This binding geometry provides a strong chemical coupling which allows for the efficient transfer of excited electrons from the adsorbed dye molecules to the substrate. N3 and the complexes studied here are ruthenium based but other dye molecules have been developed based on more common metals, such

a)Electronic mail: james.oshea@nottingham.ac.uk.

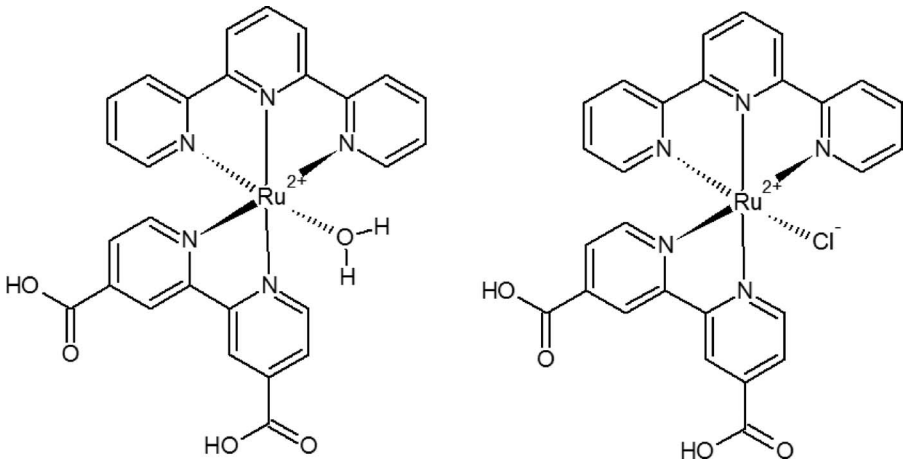

FIG. 1. Chemical structures of the single centre water splitting complex (WSC) studied in this investigation (left) and its chloride containing analog (ClSC) (right).

as copper[23,24] and organic dyes which do not need a metal centre.[25,26]

Various charge transfer studies have previously been performed on N3 molecules adsorbed on TiO_2, such as laser pump-probe techniques, which have found instrument limited charge transfer timescales of 50 fs.[27,28] Density functional theory (DFT) simulations have also been performed on this system examining the charge transfer process which predict charge transfer time scales on the order of 10 fs.[29] The core-hole clock implementation of resonant photoemission spectroscopy has revealed charge transfer can take place on the 12-16 fs time scale.[18,19] This technique will be used in a future study to determine the efficiency of charge transfer to the TiO_2 substrate for the molecules studied in this work. Here, we focus on the adsorption of the molecules to the TiO_2(110) surface and the energetics of potential charge transfer pathways.

The water splitting reaction has previously been performed using both single and multi-centre dye complexes both on surfaces and in solution.[30–34] It has been shown that multi-centre dye complexes catalyse the water splitting reaction more effectively than single centre complexes.[32] The main system studied in this work can be thought of as both a single centre water splitting complex and also as a model of the reaction centre of a multi-centre water splitting dye complex. The main dye complex investigated in this study is a single centre water splitting complex (labelled water single-centre complex or WSC) (aqua(2,2′-bipyridyl-4,4′-dicarboxylic acid)-(2,2′:6′,6″-terpyridine)Ruthenium(II)), a second complex was also investigated containing a chloride ion instead of a water molecule (labelled chloride single-centre complex or ClSC) ((2,2′-bipyridyl-4,4′-dicarboxylic acid)-(2,2′:6′,6″-terpyridine)chloride Ruthenium(II)). The chemical structures of the two dye complexes are shown in Figure 1. Dye complexes were deposited onto a rutile TiO_2 substrate at both monolayer and multilayer coverages using *in situ* ultra-high vacuum electrospray deposition. This technique has been successfully used previously to deposit carbon nanotubes,[35] C_{60} molecules,[15,36,37] zinc protoporphyrin,[38] polymers,[39] biomolecules,[40] host-guest complexes,[41] and the N3 dye complex along with related molecules.[18,19,42] The adsorbed dye molecules were studied using x-ray photoemission spectroscopy (XPS) and near-edge x-ray absorption fine structure (NEXAFS) spectroscopy in order to observe their bonding and electronic structure.

II. METHOD

Experiments were carried out at the surface science undulator beamlines I511-1 and I311 at MAX-lab, Sweden.[43,44] The I511-1 end station is equipped with a Scienta R4000 electron analyser, which can be rotated orthogonally about the beam axis. For all of the experiments in this investigation, the analyser was mounted horizontally in line with the light polarisation vector **E**, which gives the maximum flux of direct photoemission electrons. The I311 end station is equipped with a Scienta SES-200 electron analyser.

The experiments were performed using a single crystal rutile TiO_2(110) substrate (Pi-Kem, UK). Annealing was performed at I511-1 by clamping the sample to a silicon crystal and at I311 the sample was mounted on a pyrolytic boro nitride heater for annealing. Cycles of sputtering using 2 keV and 1 keV Ar^+ ions and annealing in UHV to $\sim$600 °C were used to prepare the surface. Initially, repeated cycles of sputtering and annealing were performed in order to change the crystal from an insulator to an n-type semiconductor through the introduction of bulk defects necessary to prevent sample charging. These defects, which also turn the crystal slightly blue, were minimised at the surface through annealing as described above, but nevertheless can frequently be observed as a density of states just below the conduction band edge in the valence band photoemission spectrum. The surface was determined as clean when there was a negligible C 1*s* core-level signal and a single Ti^{4+} oxidation state in the Ti 2*p* spectrum.

The two dye complexes were prepared using literature methods.[33] The dye molecules were deposited using an *in situ* UHV electrospray deposition source (MolecularSpray, UK), from a solution of $\sim$5 mg of dye in 200 ml of a

1(methanol):1(water) mixture and a pure methanol solution for the WSC and ClSC complexes, respectively. The apparatus used, and the process by which the molecules are taken from *ex situ* solution to *in situ* vacuum, are described in detail in Ref. 18. In summary, the deposition solution initially passes through a hollow stainless steel needle with a large electric field ($\sim +2$ kV) applied to it. The electric field ionizes the solution and causes the formation of a jet consisting of multiply charged droplets. These droplets then pass through a series of differentially pumped chambers towards a sample held under UHV conditions. As the droplets progress through the apparatus, they split repeatedly due to Coulomb repulsion and solvent molecules evaporate to form a molecular stream. A UHV gate valve can be used to seal off the analysis chamber from the electrospray apparatus between depositions. With the valve open but the needle voltage turned off and thus no electrospray process occurring, the pressure in the preparation chamber was $\sim 2 \times 10^{-8}$ mbar. With the voltage turned on, the preparation chamber pressure rose to $\sim 5 \times 10^{-7}$ mbar, the additional pressure being due to residual solvent molecules in the beam.

For the electron spectroscopy data, the total instrument resolution ranges from 65 to195 meV. All XPS spectra have been calibrated to the substrate O 1*s* peak at 530.05 eV,[45] and a Shirley background removed before curve fitting using Voigt functions. The NEXAFS spectra were taken over the N 1*s* absorption edge and the nitrogen Auger yield was measured using the electron analyser.

The DFT calculations were carried out as an aid to understanding the experimental data. The WSC/TiO_2(110) bonding geometry was optimized using CASTEP (Ref. 46) at the DFT-GGA level with a plane wave basis set cutoff of 260 eV and the Perdew Burke Ernzerhof functional. Atoms in the substrate were constrained to their DFT-optimized bulk lattice positions, while atoms in the molecule were unconstrained and optimized using a BFGS algorithm.

III. RESULTS AND DISCUSSION

A. Adsorption

The samples used for the following spectra are classed as either *monolayer* or *multilayer*. Here a monolayer is defined as a sample having the vast majority of molecules directly adsorbed to the surface and a multilayer as having a film of molecules thick enough that the majority of photoelectrons in XPS come from molecules above the first adsorbed layer. From the attenuation of the substrate O 1*s* XPS signal the multilayer is estimated to be at least two to three layers thick for each dye complex. The binding energies (BEs) of the peaks discussed are summarised in Table I.

Figures 2 and 3 show the O 1*s* monolayer and multilayer spectra of the WSC and ClSC dye complexes on rutile TiO_2(110), respectively. For both of the dye molecules the monolayer spectra are dominated by the TiO_2 substrate oxygen peak. The two peaks at higher binding energy are due to the oxygen atoms in the carboxylic acid groups of the bi-isonicotinic acid ligands of each molecule. For isolated dye molecules in the multilayer, the intensity of these two peaks should be equal due to the equivalent number of carbonyl (C=O) and hydroxyl (C–OH) oxygen atoms.

TABLE I. BEs (eV) for each molecule, the monolayer spectra are calibrated to the substrate O 1*s* peak at 530.05 eV and the multilayer spectra are calibrated using the Fermi level in the valence band.

		WSC	ClSC
PES			
O 1*s*	TiO_2	530.05	530.05
	Monolayer C=O and COO^-	531.3	531.3
	Multilayer C=O and COO^-	531.6	531.1
	Multilayer C-OH	533.4	533.0
C 1*s*	Terpyridine	285.3	285.3
	Bi-isonicotinic acid	286.2	286.1
	Carboxyl	288.1	288.2
Ru 3*d*		281.2	281.1
N 1*s*	Pyridine	400.3	400.5
Valence band	HOMO	2.1	2.05
N 1*s* NEXAFS			
Unshifted	LUMO	0.8	1.05
Aligned to optical data	LUMO	–0.4	–0.4

Previous studies of bi-isonicotinic acid and N3 have shown deprotonation of the hydroxyl groups on adsorption to TiO_2 to form a 2M-bidentate structure.[18,20] This is a common bonding arrangement for pyridine based molecules with carboxylic acid groups on the TiO_2 surface.[47–49] N3 is thought to bind to the surface using a single bi-isonicotinic acid ligand.[18] After deprotonation, the two oxygen atoms share an electron and are chemically equivalent. The BE of this oxygen species is similar to that of the carbonyl oxygen atom in isolated molecules and the two groups are unresolvable in the

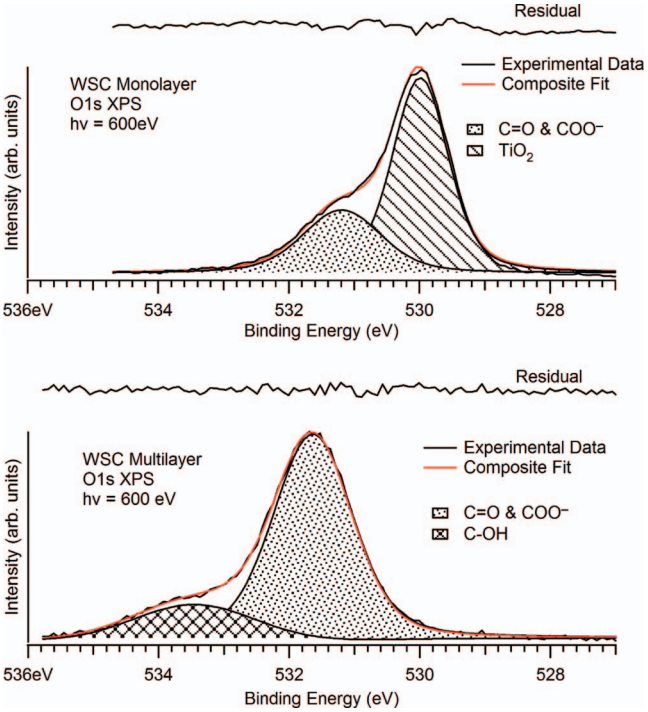

FIG. 2. O 1*s* core-level photoemission spectra of a monolayer of WSC (top) and a multilayer of WSC (bottom) on rutile TiO_2(110), measured using $h\nu = 600$ eV.

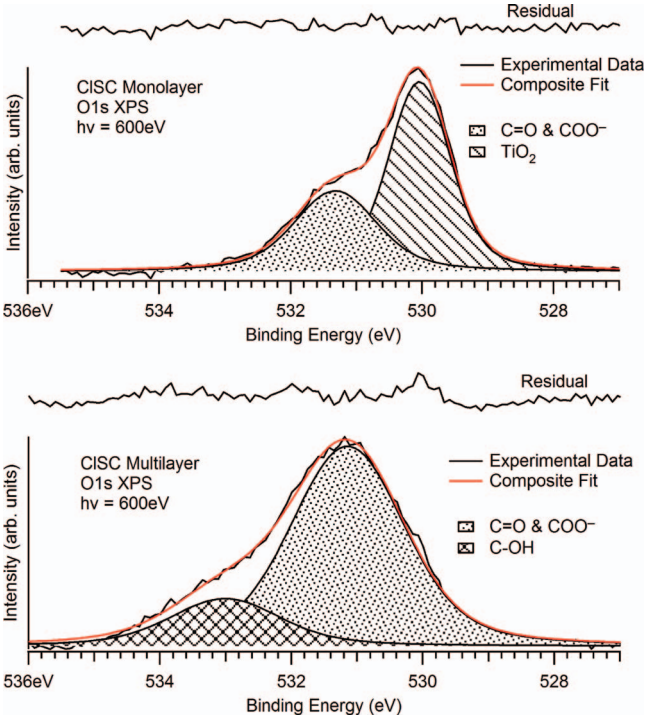

FIG. 3. O 1*s* core-level photoemission spectra of a monolayer of ClSC (top) and a multilayer of ClSC (bottom) on rutile TiO_2(110), measured using $h\nu = 600$ eV.

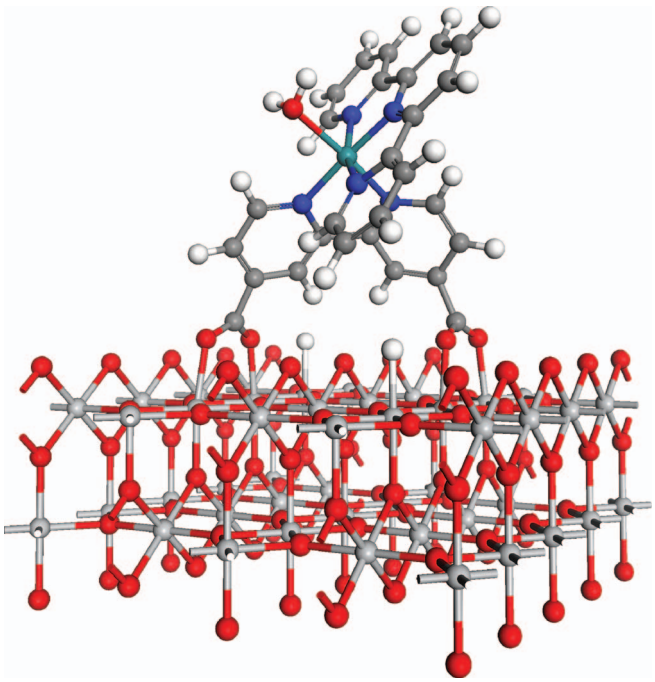

FIG. 4. The adsorption structure of the WSC complex on the rutile TiO_2(110) surface, calculated using CASTEP (Ref. 46) at the DFT-GGA level (see text for details). The different atoms are represented by: red for oxygen, blue for nitrogen, light grey for titanium, green for ruthenium, dark grey for carbon, and white for hydrogen.

XPS spectra.[20] In the monolayer spectra in Figures 2 and 3, there is no evidence of a hydroxyl oxygen peak in the WSC or ClSC spectrum. This suggests that each molecule bonds to the surface using the two available carboxylic acid groups on the bi-isonicotinic acid ligand leading to a 2M-bidentate bonding geometry on the rutile TiO_2(110) surface, in the same way as an uncomplexed bi-isonicotinic acid molecule.[20] The proposed bonding configuration for the adsorbed molecules is illustrated in Figure 4, which shows the DFT calculated structure of the WSC complex on the rutile TiO_2(110) surface.

The O 1*s* XPS spectra of multilayers of each dye complex are shown in Figures 2 and 3. A 1:1 intensity ratio of deprotonated to protonated oxygen peaks is expected on the basis of the molecular structures shown in Figure 1. The spectra show evidence of deprotonation already in the multilayer from the reduced intensity of the C–OH signal for both complexes. This is likely due to charge balance through deprotonation of the carboxylic acid groups. Previous studies on the dye complex Ru 455 have also shown proton loss when the dye was deposited under similar conditions.[19] In both the monolayer and multilayer spectra, there is no observable peak due to the oxygen atom in the water molecule, this may be because the water molecule has detached during the deposition or on adsorption to the surface or the chemical environment of the oxygen in the water molecule may be indistinguishable from the other oxygen environments.

Figure 5 shows the C 1*s* and Ru 3*d* XPS spectra of monolayers of each dye complex. The spectra appear similar and have similar BEs (as shown in Table I) for each molecule with peaks corresponding to the carbon atoms in the terpyridine and bi-isonicotinic acid ligands. Each spectrum is dominated by a peak due to the carbon atoms in the pyridine groups. Also present at higher BE is the peak due to the carbon atom in the carboxylic acid groups. There are also two peaks due to the central ruthenium ion as the Ru 3*d* state is a doublet

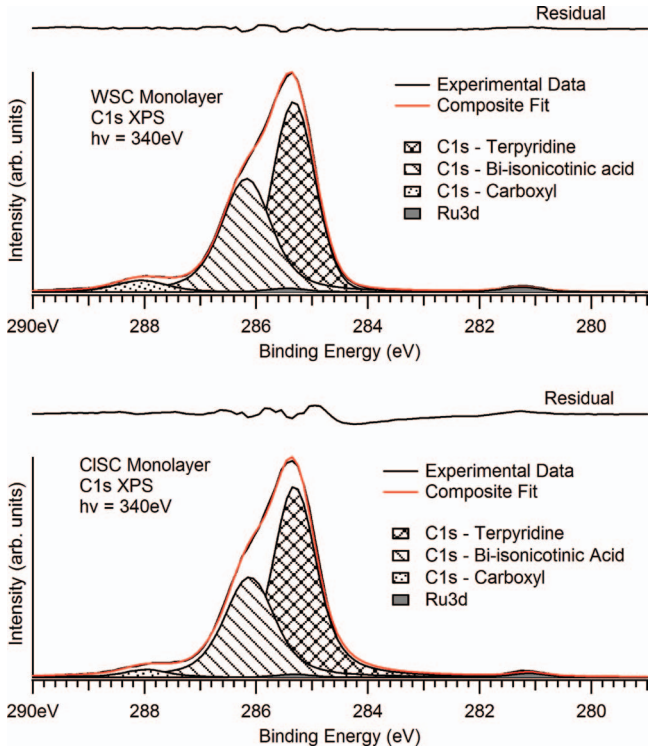

FIG. 5. C 1*s* and Ru 3*d* core-level photoemission spectra of monolayers of WSC (top) and ClSC (bottom) on rutile TiO_2(110), measured using $h\nu = 340$ eV.

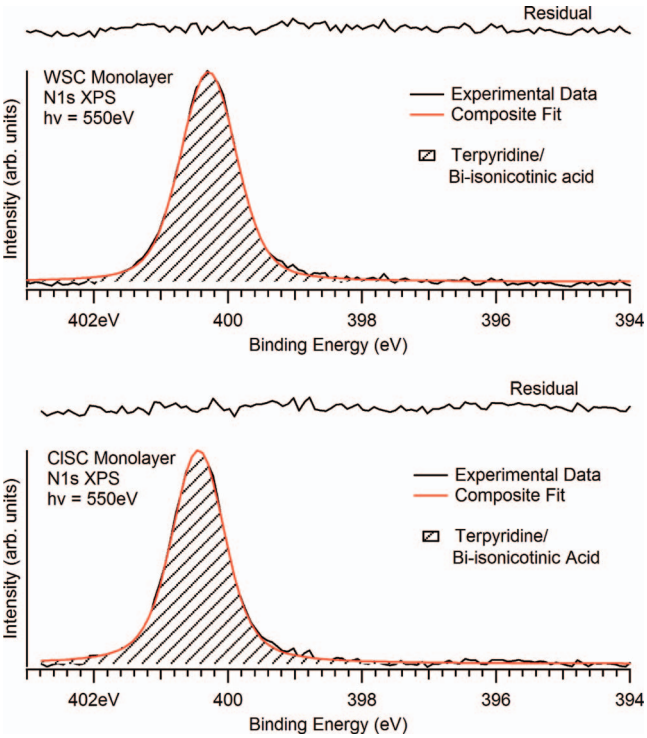

FIG. 6. N 1*s* core-level photoemission spectra of monolayers of WSC (top) and ClSC (bottom) on rutile TiO_2(110), measured using h$\nu = 550$ eV.

state with a spin orbit splitting of 4.2 eV.[50] The lower BE Ru $3d_{5/2}$ peak is present at ∼281 eV. This is ∼1 eV higher than metallic ruthenium,[50] consistent with the Ru^{2+} oxidation state of the metal centre.

Figure 6 shows the N 1*s* XPS spectra of monolayers of each dye complex. Both dye complexes show only a single nitrogen peak as expected from their chemical structure corresponding to the nitrogen atoms in the pyridine rings. This supports the other photoemission data discussed indicating that the molecules have retained their molecular integrity during deposition.

Figure 7 shows the Cl 2*p* XPS spectrum of a monolayer of the ClSC dye complex, the multilayer spectrum is not shown as it has a similar appearance to the monolayer spectrum. The spectrum consists of two peaks which are due to Cl

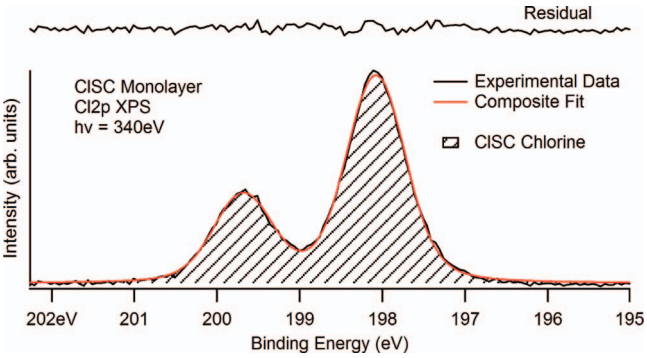

FIG. 7. Cl 2*p* core-level photoemission spectrum of a monolayer ClSC on rutile TiO_2(110), measured using h$\nu = 340$ eV.

2*p* being a doublet state. The state has a spin-orbit splitting of ∼1.65 eV. The lower BE peak is present at ∼198 eV.

B. Electronic structure

In a DSC, electrons are photoexcited from high-lying occupied molecular orbitals to previously unoccupied molecular orbitals. For subsequent electron injection into the substrate, the unoccupied level in question must overlap with available states in the substrate conduction band. Spectra representing the occupied and unoccupied states of monolayers of each dye complex have here been placed on a common BE scale as shown in Figure 9, following a procedure outlined in Ref. 51. This procedure has previously been performed on monolayers of N3 and related molecules.[18,19] The resulting energy level alignment diagrams can be used to identify the potential charge transfer processes that can occur in the dye complexes.[16,17,52,53]

The UV/visible light spectra of the WSC and ClSC dye complexes in solution are shown in Figure 8. A real solar cell device will operate using optical excitation producing valence-holes in the molecules, this is in contrast to the core-holes created by the x rays used for the photoemission and NEXAFS measurements. The lowest energy maximum in each spectrum is attributed to the HOMO → LUMO transition corresponding to a metal-to-ligand charge transfer (MLCT) Ru(4d) → bpy(π*)COOH transition. The energy of this excitation is lower for the ClSC dye than the WSC dye.

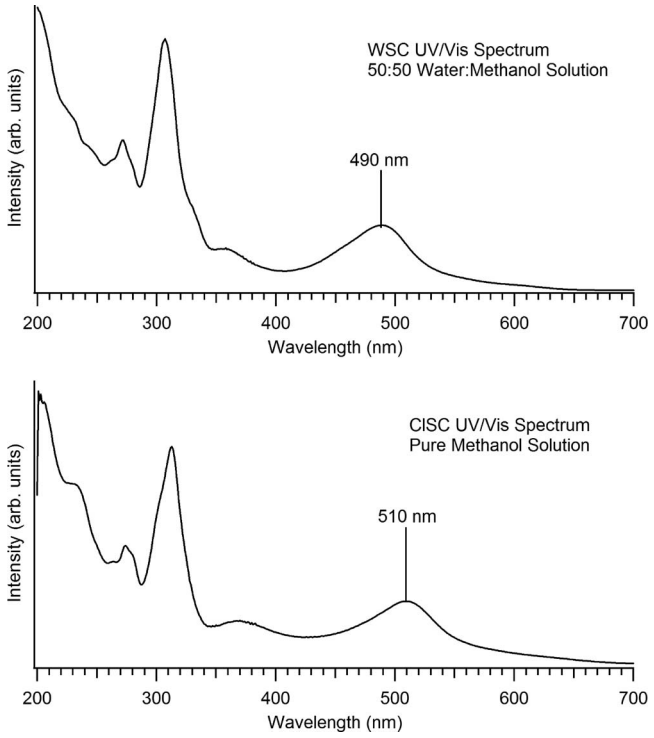

FIG. 8. Optical absorption spectra of the WSC and ClSC complexes in solution. The spectra were taken over the visible light and ultraviolet wavelength range, the wavelengths corresponding to the lowest energy absorption maxima are labelled on the spectra.

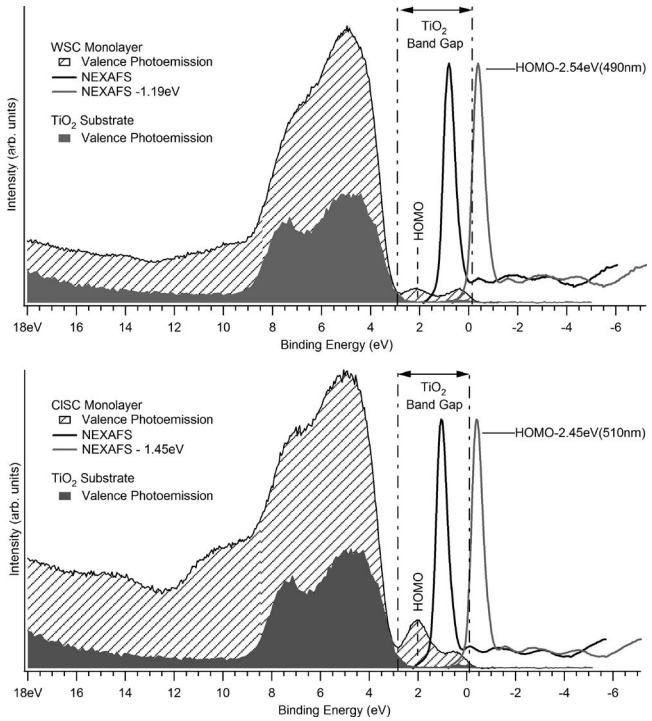

FIG. 9. Valence band photoemission spectra of the clean substrate and of a monolayer of dye molecule, adjacent to a N 1*s* NEXAFS spectrum of the monolayer. The NEXAFS spectra are also shown shifted to align with the relevant optical HOMO-LUMO gap (shown in a lighter shade and labelled with the position of the measured HOMO minus the energy of the optical absorption). The photoemission spectra were measured using hν = 60 eV. The NEXAFS spectra were taken over the photon energy range hν = 398–406 eV.

Figure 9 shows the N 1*s* (Auger yield) NEXAFS and valence photoemission spectra for a monolayer of each dye complex, along with the clean substrate valence photoemission spectrum (measured at hν =110 eV). The N 1*s* core level XPS spectra showed only a single pyridine based nitrogen peak for both complexes, this peak was used to place the NEXAFS on the common BE axis. Previous studies on the bi-isonicotinic acid ligand and on the N3 dye complex have shown that the N 1*s* NEXAFS is dominated by pyridine-like π^* orbitals.[18,54,55]

The valence band spectra for monolayers of WSC and ClSC molecules appear similar to those previously obtained for monolayers of N3 and related molecules.[18,19] The lowest binding energy molecular peak in the valence photoemission spectra corresponds to the HOMO. The peak at lower binding energy is due to the substrate defect gap state, which is introduced when turning the substrate into a semiconductor as described in the Method section previously. For each dye complex, the HOMO is present within the substrate bandgap which prevents back transfer of electrons from the substrate. The ClSC HOMO appears to have greater intensity than that of the WSC HOMO, this effect may be due to differences in coverage between the samples studied. The HOMO is located at a BE of 2.1 and 2.05 eV for the WSC and ClSC dye complexes, respectively. The HOMO of each of these dye complexes is located at higher BE than for those reported for models of the charge transfer centres of a multi-centre water splitting dye complex (1.3–1.9 eV).[19] After charge transfer from the molecules to the substrate has occurred, this could create a large potential to remove electrons from an attached water molecule.

In the present case where the unoccupied states are probed using N 1*s* NEXAFS, a *core* exciton (bound electron-hole pair) is created, whereas in an optically excited system a *valence* exciton is created. The presence of a hole shifts the unoccupied states to higher binding energy with respect to the ground state. The BE of the excitons, equivalent to the amount by which the unoccupied levels shift, is attributed to a combination of the Coulomb interaction between the hole and the excited electron and the rehybridization of the molecular states upon core- or valence-hole creation.[56] Comparing the HOMO-LUMO gap for optical excitation (2.54 and 2.45 eV) to the HOMO-LUMO gap for the core-excited system (1.3 and 1 eV), the difference in energy is 1.2 and 1.45 $\pm$ 0.1 eV for the WSC and ClSC dye complexes, respectively (assuming a minimal effect from the solvent in the optical measurements). This is indicative of the difference between the N 1*s* core exciton and valence exciton BEs for the molecules. These values are consistent with the difference in BE found for pyridine,[56] a molecule closely related to the bi-isonicotinic acid ligands of the dye complexes, especially concerning the chemical environment of the nitrogen atoms being probed here. Similar results for the difference in exciton BEs have previously been found for bipyridine based dye complexes, such as N3.[18,19]

Shifting the NEXAFS spectra of each dye complex into line with the optical HOMO-LUMO gap, as shown in Figure 9, causes the LUMO to lie above the conduction band edge. In a real water splitting device, this energetic overlap permits electron injection from the LUMO into the substrate for both dye complexes. The presence of a core exciton in the NEXAFS causes the LUMO of the core-excited systems to lie within the substrate bandgap preventing charge transfer for this orbital.

IV. CONCLUSIONS

The UHV electrospray deposition has been used to deposit monolayers and multilayers of the WSC and ClSC dye complexes on the rutile TiO_2(110) surface *in situ*. Photoemission spectroscopy has been used to characterize the core and valence levels of the system, which were used to deduce the bonding geometry of each dye complex on the rutile TiO_2(110) surface. We find that for both dye complexes carboxylic acid groups deprotonate so that their O atoms bond to Ti atoms on the substrate surface, this would suggest that the complexes adopt a 2M-bidentate bonding geometry on the rutile TiO_2(110) surface.

The energetic alignment of the system was determined by placing the valence photoemission and N 1*s* NEXAFS of a monolayer of each dye complex onto a common BE scale. The bandgap of TiO_2(110) was aligned using the valence photoemission of the clean substrate. The optical absorption maximum for each dye complex was attributed to the HOMO $\rightarrow$ LUMO transition in a working solar cell. This was used to compare the energetics as they would appear for

photoexcitation from the valence band (as occurs in working DSCs) with those found for photoexcitation from the N 1*s* core level, for which the unoccupied levels appear at higher BE. This comparison allowed quantification of the difference in BE of a core and valence excitation for each dye complex system, found to be 1.2 and 1.45 ± 0.1 eV. for the WSC and ClSC dye complexes, respectively. The energetic alignments reveal that the LUMO of each dye complex is incapable of charge transfer to the substrate when a core exciton is created, after optical excitation both dye complexes are capable of charge transfer from their LUMO while adsorbed on the rutile TiO_2(110) surface. This information will be used in future experiments to determine charge transfer time scales of both dye complexes. This shows that rutile TiO_2(110) could be an appropriate substrate for a single centre water splitting DSC.

The valence band photoemission spectra show that the HOMO of the WSC and ClSC dye complexes occur at far higher BE than those previously seen for the N3 dye complex and related molecules each of which contains two or more bipyridine-based ligands.[18,19] The information obtained from these experiments will be used in the design of a multi-centre water splitting DSC.

ACKNOWLEDGMENTS

We are grateful for financial support by the European Community – Research Infrastructure Action under the FP6 "Structuring the European Research Area" Programme (through the Integrated Infrastructure Initiative "Integrating Activity on Synchrotron and Free Electron Laser Science"), the UK Engineering and Physical Sciences Research Council (EPSRC). We express our thanks to the staff of MAX-lab for their technical assistance, especially Dr. A. Pietzsch and Dr. K. Schulte and also to Dr. J. Schnadt of the Division of Synchrotron Radiation Research, Lund University for the loan of his electrospray deposition source. N.R.C. gratefully acknowledges receipt of a Royal Society Leverhulme Trust Senior Research Fellowship.

[1] L. Schlapbach and A. Züttel, Nature (London) **414**, 353 (2001).
[2] A. C. Dillon, K. M. Jones, T. A. Bekkedahl, C. H. Kiang, D. S. Bethune, and M. J. Heben, Nature (London) **386**, 377 (1997).
[3] C. Liu, Y. Y. Fan, M. Liu, H. T. Cong, H. M. Cheng, and M. S. Desselhaus, Science **286**, 1127 (1999).
[4] N. L. Rosi, J. Eckert, M. Eddaoudi, D. T. Vodak, J. Kim, M. O'Keefe, and O. M. Yaghi, Science **300**, 1127 (2003).
[5] S. H. Yang, X. Lin, A. J. Blake, G. S. Walker, P. Hubberstey, N. R. Champness, and M. Schröder, Nature Chem. **1**, 487 (2009).
[6] X. Lin, I. Telepeni, A. J. Blake, A. Dailly, C. M. Brown, J. M. Simmons, M. Zoppi, G. S. Walker, K. M. Thomas, T. J. Mays, P. Hubberstey, N. R. Champness, and M. Schröder, J. Am. Chem. Soc. **131**, 2159 (2009).
[7] S. Cheng and B. E. Logan, Proc. Natl. Acad. Sci. U.S.A. **104**, 18871 (2007).
[8] D. K. Liguras, D. I. Kondarides, and X. E. Verykios, Appl. Catal., B **43**, 345 (2003).
[9] A. F. Ghenciu, Curr. Opin. Solid State Mater. Sci. **6**, 389 (2002).
[10] M. Grätzel and A. Hagfeldt, Acc. Chem. Res. **33**, 269 (2000).
[11] M. Grätzel, Nature (London) **414**, 338 (2001).
[12] M. Grätzel, J. Photochem. Photobiol. C **4**, 145 (2003).
[13] M. Grätzel, Nature (London) **421**, 586 (2003).
[14] E. W. McFarland and J. Tang, Nature (London) **421**, 616 (2003).
[15] A. J. Britton, A. Rienzo, K. Schulte, and J. N. O'Shea, J. Chem. Phys. **113**, 094705 (2010).
[16] J. B. Taylor, L. C. Mayor, J. C. Swarbrick, J. N. O'Shea, C. Isvoranu, and J. Schnadt, J. Chem. Phys. **127**, 134707 (2007).
[17] J. Schnadt, P. A. Brühwiler, L. Patthey, J. N. O'Shea, S. Södergren, M. Odelius, R. Ahuja, O. Karis, M. Bässler, P. Persson, H. Siegbahn, S. Lunell, and N. Mårtensson, Nature (London) **418**, 620 (2002).
[18] L. C. Mayor, J. B. Taylor, G. Magnano, A. Rienzo, C. J. Satterley, J. N. O'Shea, and J. Schnadt, J. Chem. Phys. **129**, 114701 (2008).
[19] M. Weston, A. J. Britton, and J. N. O'Shea, J. Chem. Phys. **134**, 054705 (2011).
[20] L. Patthey, H. Rensmo, P. Persson, K. Westermark, L. Vayssieres, A. Stashans, Å. Petersson, P. A. Brühwiler, H. Siegbahn, S. Lunell, and N. Mårtensson, J. Chem. Phys. **110**, 5913 (1999).
[21] M. Grätzel, J. Photochem. Photobiol. A **164**, 3 (2004).
[22] E. M. J. Johansson, M. Hedlund, H. Siegbahn, and H. Rensmo, J. Phys. Chem. B **109**, 22256 (2005).
[23] A. H. Rendondo, E. C. Constable, and C. E. Housecroft, Chimia **63**, 205 (2009).
[24] E. C. Constable, A. H. Rendondo, C. E. Housecroft, M. Neuburger, and S. Schaffner, Dalton Trans. **33**, 6634 (2009).
[25] M. Hahlin, E. M.J. Johansson, S. Plogmaker, M. Odelius, D. P. Hagberg, L. Sun, H. Siegbahn, and H. Rensmo, Phys. Chem. Chem. Phys. **12**, 1507 (2010).
[26] T. Marinado, M. Hahlin, X. Jiang, M. Quintana, E. M. J. Johansson, E. Gabrielsson, S. Plogmaker, D. P. Hagberg, G. Boschloo, S. M. Zakeeruddin, M. Grätzel, H. Siegbahn, L. Sun, A. Hagfeldt, and H. Rensmo, J. Phys. Chem. C **114**, 11903 (2010).
[27] R. J. Ellingson, J. B. Asbury, S. Ferrere, H. N. Ghosh, J. R. Sprague, T. Q. Lian, and A. J. Nozik, J. Phys. Chem. B **102**, 34 (1998).
[28] J. B. Asbury, R. J. Ellingson, H. N. Ghosh, S. Ferrere, A. J. Nozik, and T. Q. Lian, J. Phys. Chem. B **103**, 3110 (1999).
[29] P. Persson and M. J. Lundqvist, J. Phys. Chem. B **109**, 11918 (2005).
[30] J. Concepcion, J. W. Jurss, M. R. Norris, Z. F. Chen, J. L. Templeton, and T. J. Meyer, Inorg. Chem. **49**, 1277 (2010).
[31] J. Concepcion, J. W. Jurss, J. L. Templeton, and T. J. Meyer, J. Am. Chem. Soc. **49**, 16462 (2008).
[32] J. Concepcion, J. W. Jurss, M. K. Brennaman, P. G. Hoertz, A. O. T. Patrocinio, N. Y. M. Iha, J. L. Templeton, and T. J. Meyer, Acc. Chem. Res. **42**, 1954 (2009).
[33] D. J. Wasylenko, C. Ganesamoorthy, B. D. Kolvisto, M. A. Henderson, and C. P. Berlinguette, Inorg. Chem. **49**, 2202 (2010).
[34] D. J. Wasylenko, C. Ganesamoorthy, M. A. Henderson, B. D. Kolvisto, H. D. Osthoff, and C. P. Berlinguette, J. Am. Chem. Soc. **132**, 16094 (2010).
[35] J. N. O'Shea, J. B. Taylor, J. C. Swarbrick, G. Magnano, L. C. Mayor, and K. Schulte, Nanotechnology **18**, 035707 (2007).
[36] A. Saywell, G. Magnano, C. J. Satterley, L. M. A. Perdigao, N. R. Champness, P. H. Beton, and J. N. O'Shea, J. Phys. Chem. **112**, 7706 (2008).
[37] C. J. Satterley, L. M. A. Perdigao, A. Saywell, G. Magnano, A. Rienzo, L. C. Mayor, V. R. Dhanak, P. H. Beton, and J. N. O'Shea, Nanotechnology **18**, 455304 (2007).
[38] A. Rienzo, L. C. Mayor, G. Magnano, C. J. Satterley, E. Ataman, J. Schnadt, and J. N. O'Shea, J. Chem. Phys. **132**, 084703 (2010).
[39] J. E. Lyon, A. J. Cascio, M. M. Beerborn, R. Schlaf, Y. Zhu, and S. A. Jenekhe, Appl. Phys. Lett. **88**, 222109 (2006).
[40] S. Rauschenbach, F. L. Stadler, E. Lunedei, N. Malinowski, S. Koltsov, G. Costantini, and K. Kern, Small **2**, 540 (2006).
[41] N. Thontasen, G. Levita, N. Malinowski, Z. Deng, S. Rauschenbach, and K. Kern, J. Phys. Chem. C **114**, 17768 (2010).
[42] L. C. Mayor, A. Saywell, G. Magnano, C. J. Satterley, J. Schnadt, and J. N. O'Shea, J. Chem. Phys. **130**, 164704 (2009).
[43] R. Denecke, P. Vaterlein, M. Bassler, N. Wassdahl, S. Butorin, A. Nilsson, J. E. Rubensson, J. Nordgren, N. Martensson, and R. Nyholm, J. Electron Spectrosc. Relat. Phenom. **103**, 971 (1999).
[44] R. Nyholm, J. N. Andersen, U. Johansson, B. N. Jensen, and I. Lindau, J. Electron Spectrosc. Relat. Phenom. **467–468**, 520 (2001).
[45] J. Schnadt, J. N. O'Shea, L. Patthey, J. Schiessling, J. Krempaský, M. Shi, J. Schiessling, N. Mårtensson, and P. A. Brühwiler, Surf. Sci. **544**, 74 (2003).
[46] M. D. Segall, P. J. D. Lindan, M. J. Probert, C. J. Pickard, P. J. Hasnip, S. J. Clark, and M. C. Payne, J. Phys.: Condens. Matter **14**, 2717 (2002).

[47]J. N. O'Shea, Y. Luo, J. Schnadt, L. Patthey, H. Hillesheimer, J. Krempaský, D. Nordlund, M. Nagasono, and N. Mårtensson, Surf. Sci. **486**, 157 (2001).
[48]J. N. O'Shea, J. Schnadt, P. A. Brühwiler, and H. H. N. Mårtensson, J. Phys. Chem. B **105**, 1917 (2001).
[49]J. N. O'Shea, J. C. Swarbrick, K. Nilson, C. Puglia, B. Brena, Y. Luo, and V. Dhanak, J. Chem. Phys. **121**, 10203 (2004).
[50]J. C. Fuggle and N. Mårtensson, J. Electron Spectrosc. Relat. Phenom. **21**, 275 (1980).
[51]J. Schnadt, J. N. O'Shea, L. Patthey, J. Krempaský, N. Mårtensson, and P. A. Brühwiler, Phys. Rev. B **67**, 235420 (2003).
[52]J. B. Taylor, L. C. Mayor, J. C. Swarbrick, J. N. O'Shea, and J. Schnadt, J. Phys. Chem. C **111**, 16646 (2007).
[53]J. Schnadt, J. N. O'Shea, L. Patthey, L. Kjeldgaard, J. Åhlund, K. Nilson, J. Schiessling, J. Krempaský, M. Shi, O. Karis, C. Glover, H. Siegbahn, N. Mårtensson, and P. A. Brühwiler, J. Chem. Phys. **119**, 12462 (2003).
[54]P. Persson, S. Lunell, P. A. Brühwiler, J. Schnadt, S. Södergren, J. N. O'Shea, O. Karis, H. Siegbahn, N. Mårtensson, M. Bässler, and L. Patthey, J. Chem. Phys. **112**, 3945 (2000).
[55]J. N. O'Shea, J. B. Taylor, L. C. Mayor, J. C. Swarbrick, and J. Schnadt, Surf. Sci. **602**, 1693 (2008).
[56]J. Schnadt, J. Schiessling, and P. A. Brühwiler, Chem. Phys. **312**, 39 (2005).